



Transmission dynamics of Monkeypox virus: a mathematical modelling approach

Olumuyiwa James Peter¹ · Sumit Kumar² · Nitu Kumari² · Festus Abiodun Oguntolu³ · Kayode Oshinubi⁴ · Rabi Musa⁵

Received: 21 July 2021 / Accepted: 30 September 2021 / Published online: 15 October 2021
© The Author(s), under exclusive licence to Springer Nature Switzerland AG 2021

Abstract

Monkeypox (MPX), similar to both smallpox and cowpox, is caused by the monkeypox virus (MPXV). It occurs mostly in remote Central and West African communities, close to tropical rain forests. It is caused by the monkeypox virus in the Poxviridae family, which belongs to the genus Orthopoxvirus. We develop and analyse a deterministic mathematical model for the monkeypox virus. Both local and global asymptotic stability conditions for disease-free and endemic equilibria are determined. It is shown that the model undergo backward bifurcation, where the locally stable disease-free equilibrium co-exists with an endemic equilibrium. Furthermore, we determine conditions under which the disease-free equilibrium of the model is globally asymptotically stable. Finally, numerical simulations to demonstrate our findings and brief discussions are provided. The findings indicate that isolation of infected individuals in the human population helps to reduce disease transmission.

Keywords Monkeypox virus · Mathematical model · Stability · Backward bifurcation

Introduction

Monkeypox is a severe viral zoonotic disease (i.e., animal-to-human infection) that occurs sporadically, primarily in rural areas in Central and Western Africa, near tropical rainforests. This is caused by the monkeypox virus within the Poxviridae family that belongs to the genus Orthopoxvirus (Durski et al. 2018; Jezek et al. 1988). The genus Orthopoxvirus also comprises variola virus (the origin of smallpox), vaccinia virus (used for the eradication of smallpox in the vaccine), and cowpox virus (used in the earlier vaccine).

Monkeypox virus is mainly transmitted to humans from wild animals such as rodents and primates, but transmission often occurs from humans to humans. Human to human transmission has been linked to respiratory droplets and contact with bodily fluids, a contaminated patient's environment or items, and a skin lesion on an infected individual (Alakunle et al. 2020). Monkeypox virus has emerged as the most common orthopox virus after the eradication of the smallpox (Kantele et al. 2016). Fever, headache, muscle aches, backache, swollen lymph nodes, chills, and weariness are some of the symptoms that some individuals who may have contracted monkeypox experience. Up to a tenth of those infected with monkeypox die, with the majority of deaths happening in children under the age of ten (Nguyen et al. 2021).

Monkeypox was identified in 1958 when two pox-like disease outbreaks occurred in monk colonies held for study, hence the term 'monkeypox'. The first human case was reported in the Democratic Republic of Congo in 1970 during a time of increased attempts to eradicate the smallpox. Among other Central and Western African countries like Cameroon, Gabon, Cote d'Ivoire, Liberia, Central African Republic, Congo, South Sudan and Sierra Leone, monkeypox has since been identified in humans. The first proof of

✉ Olumuyiwa James Peter
peterjames4real@gmail.com

¹ Department of Mathematics, University of Ilorin, Ilorin, Nigeria

² School of Basic Sciences, Indian Institute of Technology Mandi, Mandi, Himachal Pradesh 175001, India

³ Department of Mathematics, Federal University of Technology Minna, Minna, Nigeria

⁴ AGIES Research Unit, Universite Grenoble Alpes, Alpes, France

⁵ School of Mathematics, Statistics and Computer Science, University of KwaZulu-Natal, Durban, South Africa

monkeypox outbreaks in humans outside of Africa was a 2003 outbreak in the US. Monkeypox importation was later recognized in the United Kingdom and Israel. Mortality rate ranged from 1 percent to 10 percent in occurrences, with most deaths arising in younger populations (Ladnyj et al. 1972; CDC 2003). Monkeypox's incubation period is typically about 6–16 days but can vary from 5 to 21 days. There are two facets of the contagious era, with an initial intrusive duration in the first 5 days, where the main signs are fever, lymphadenopathy (lymph node swelling), back pain, extreme headache, myalgia (muscle ache) and serious asthenia (energy shortage). A maculopapular rash (flat-based skin lesions) occurs 1–3 days after the onset of fever, and grows into small fluid-filled blisters (vesicles), which are pus-filled and then crust over in about ten days (Hutson et al. 2013).

Presently, there are no clear treatments available for monkeypox infection, though numerous novel antivirals, such as Brincidofovir, Tecovirimat and vaccinia immune globulin can be used to control the spread of the disease. There has been a significant increase in monkeypox in the last decade, associated with the decrease in herd immunity to smallpox. Vaccination against smallpox has been shown to be successful at 85 percent in the prevention of monkeypox but is no longer regularly available since global eradication of smallpox. The post-exposure vaccine can help prevent or decrease the severity of the disease (Rimoin et al. 2010; Meyer et al. 2020).

The disease has been given little attention in the past and this has contributed to insufficient knowledge on its mechanisms of transmission. Nevertheless, few studies have tried to research dynamics of monkeypox virus using a mathematical modelling technique. Study in Bhunu and Mushayabasa (2011) provides the basis for transmission analysis of pox-like dynamics of monkeypox virus as a case study. In Bhunu et al. (2009), the authors have shown that with the planned treatment intervention, the disease will be eradicated from both human and non-human primates in due time. The dynamics of monkeypox virus in human host and rodent with the stability analysis is studied in Usman and Adamu (2017). Other significant contributions can be found in TeWinkel (2019), Somma et al. (2019), Bankuru et al. (2020), Grant et al. (2020). Having gone through several works on the monkeypox virus and its mechanisms of transmission, we found that none considered the combination of isolated, exposed compartments in the human subpopulation and the effects of that contact rate with rodent population. Our aim is to investigate the various factors that could lead to reduction in the disease

transmission and the effects of such factors on the basic reproduction number.

The rest of this paper is structured as follows: Method which includes model formulation and analysis are described in “Method” section. Next, “Backward bifurcation” section consists of the numerical simulations and results, discussion of results is given in “Results”, “Discussion” sections. Finally, in “Conclusion” section, we have provided conclusions of this article. Table 1 shows a detailed description of the parameters, while the model's compartmental flow diagram is shown in Fig. 1.

Method

We propose a deterministic compartmental model on the transmission dynamics of monkeypox consisting of two populations that is, humans and rodents. The human population is further subdivided into five compartments, susceptible humans $S_h(t)$, exposed humans $E_h(t)$, infected humans $I_h(t)$, isolated humans $Q_h(t)$ and recovered humans $R_h(t)$. The rodent population is subdivided into three compartments, susceptible rodents $S_r(t)$, exposed rodents $E_r(t)$ and infected rodents $I_r(t)$. Recruitment into human population is at a rate θ_h . β_1 is the effective contact rate with the probability of human been infected with the virus per contact with an infected rodent and β_2 is the product of effective contact rate and the probability of human been infected with monkey pox virus after getting in contact with infectious human. The proportion of exposed individuals moving to highly infected class is α_2 while the proportion identified is α_1 . After medical diagnosis, some suspected cases are confirmed, where others were not detected and returned back to susceptible humans a rate φ . The suspected cases are treated and moved to recovered class at a rate τ . The recovery rate for human is at a rate γ . Natural death occurs in the humans and rodents population at the rates μ_h and μ_r respectively. β_3 is the effective contact rate with the probability of rodent been infected per contact with infected rodent. The infected rodent population decreased by natural mortality rate μ_r or by disease induced death rate δ_r . The transition among various compartments considered in the model is illustrated in Fig. 1, the model is governed by the following set of nonlinear differential equations below:

Fig. 1 Schematic representation of the model

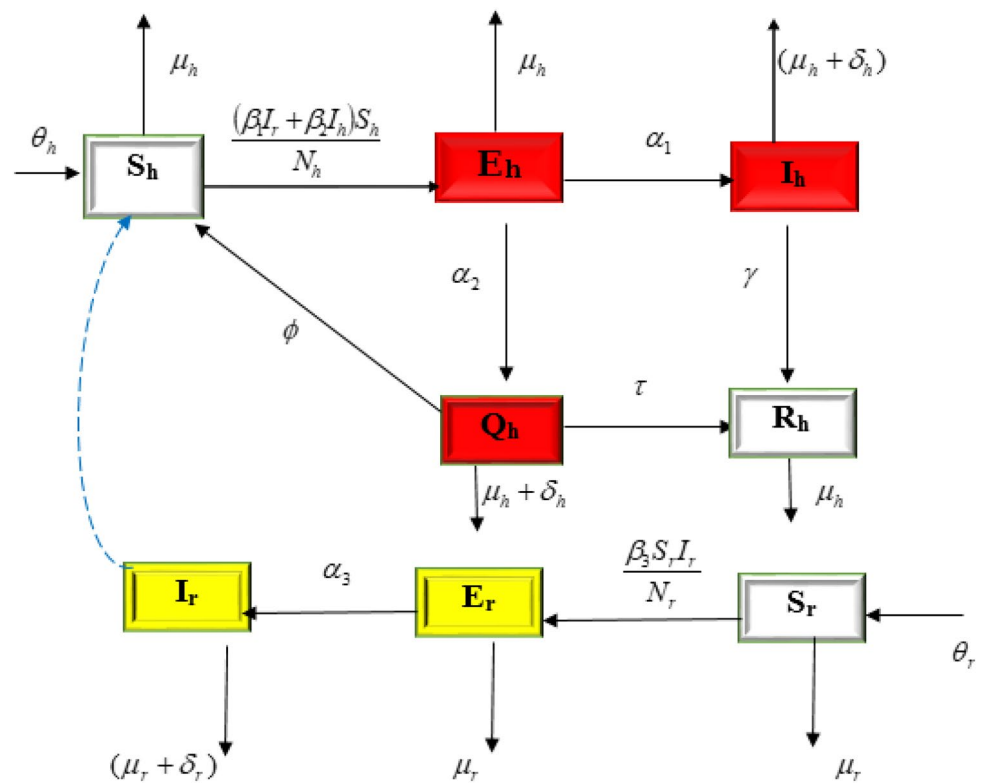


Table 1 Parameter values used for the simulations

Parameter	Value, Year ⁻¹	Source	Description
θ_h	0.029	Bhunu et al. (2009)	Recruitment rate for humans
θ_r	0.2	Bhunu et al. (2009)	Recruitment rate for rodents
β_1	0.00025	Bhunu and Mushayabasa (2011)	Rodent contact rate to humans
β_2	0.00006	Bhunu and Mushayabasa (2011)	Human to humans contact rate
β_3	0.027	Bhunu and Mushayabasa (2011)	Rodent to rodent contact rate
α_1	0.2	Assumed	Proportion of exposed human to infected humans
α_2	2.0	Estimated	Proportion identified as suspected case
ϕ	2.0	Estimated	Proportion not detected after diagnosis
τ	0.52	Assumed	Progression from isolated to recovered class
γ	0.83	Bhunu et al. (2009)	Humans recovery rate
μ_h	1.5	Bhunu and Mushayabasa (2011)	Natural death rate of human
μ_r	0.002	Bhunu and Mushayabasa (2011)	Natural death rate of rodents
δ_r	0.5	Assumed	Disease induced death rate for rodents
δ_h	0.2	Odom et al. (2009)	Disease induced death rate for humans

$$\begin{aligned}
 \frac{dS_h}{dt} &= \theta_h - \frac{(\beta_1 I_r + \beta_2 I_h) S_h}{N_h} - \mu_h S_h + \varphi Q_h \\
 \frac{dE_h}{dt} &= \frac{(\beta_1 I_r + \beta_2 I_h) S_h}{N_h} - (\alpha_1 + \alpha_2 + \mu_h) E_h \\
 \frac{dI_h}{dt} &= \alpha_1 E_h - (\mu_h + \delta_h + \gamma) I_h \\
 \frac{dQ_h}{dt} &= \alpha_2 E_h - (\varphi + \tau + \delta_h + \mu_h) Q_h \\
 \frac{dR_h}{dt} &= \gamma I_h + \tau Q_h - \mu_h R_h \\
 \frac{dS_r}{dt} &= \theta_r - \frac{\beta_3 S_r I_r}{N_r} - \mu_r S_r \\
 \frac{dE_r}{dt} &= \frac{\beta_3 S_r I_r}{N_r} - (\mu_r + \alpha_3) E_r \\
 \frac{dI_r}{dt} &= \alpha_3 E_r - (\mu_r + \delta_r) I_r
 \end{aligned}
 \tag{1}$$

The model analysis

For the human population, $N_h = S_h + E_h + I_h + Q_h + R_h$, the differential equation is given as:

$$(dN_h)/dt = \theta_h - \delta_h I_h - \mu_h N_h \tag{2}$$

Also, for the rodent population

$N_r = S_r + E_r + I_r$, and the corresponding differential equations is given as:

$$(dN_r)/dt = \theta_r - (\mu_r + \theta_r) N_r \tag{3}$$

Theorem 1 *Let $(S_h, E_h, I_h, Q_h, R_h, S_r, E_r, R)$ be the solution of 1 with the initial conditions in a biologically feasible region $\Gamma = \Gamma_h \times \Gamma_r$ with:*

$$\Gamma_h = S_h, E_h, I_h, Q_h, R_h \in R_+^5 : N_h \leq \frac{\theta_h}{\mu_h} \tag{4}$$

and

$$\Gamma_r = S_r, E_r, R_r \in R_+^3 : N_r \leq \frac{\theta_r}{\mu_r} \tag{5}$$

Then Γ is non-negative invariant

Following the approach of Somma et al. (2019), we have that:

$$0 \leq N_h(t) \leq N_h(0) e^{-\mu_h t} + \frac{\theta_h}{\mu_r} (1 - e^{-\mu_h t}) \tag{6}$$

also

$$N_r(t) \leq N_r(0) e^{-(\mu_r + \theta)t} + \frac{\theta_r}{\mu_r} (1 - e^{-(\mu_r + \theta)t}) \tag{7}$$

Hence, the set Γ is positive invariant and for t .

Monkeypox-free equilibrium state

This occurs in the absence of disease. Thus, in the absence of infection, we set E_h, I_h, Q_h, R_h, E_r and I_r to zero in 1 and the resulting solution gives the monkeypox-free equilibrium states given as:

$$\Phi_{MFE} (S_h^*, E_h^*, I_h^*, Q_h^*, R_h^*, S_r^*, E_r^*, I_r^*) \tag{8}$$

Endemic equilibrium

This occurs when the infection persist in the population represented by $\Phi_{MEE} (S_h^*, E_h^*, I_h^*, Q_h^*, R_h^*, S_r^*, E_r^*, I_r^*)$. Thus,

$$\begin{aligned}
 S_h^* &= \frac{k_1 k_3 \theta_h}{\mu_h k_1 k_3 - \alpha_2 \varphi \phi_h + k_1 k_3 \phi_h} \\
 E_h^* &= \frac{k_3 \phi_h \theta_h}{\mu_h k_1 k_3 - \alpha_2 \varphi \phi_h + k_1 k_3 \phi_h} \\
 I_h^* &= \frac{k_3 \alpha_1 \phi_h \theta_h}{k_2 (\mu_h k_1 k_3 - \alpha_2 \varphi \phi_h + k_1 k_3 \phi_h)} \\
 Q_h^* &= \frac{\alpha_2 \phi_h \theta_h}{\mu_h k_1 k_3 - \alpha_2 \varphi \phi_h + k_1 k_3 \phi_h} \\
 R_h^* &= \frac{(\alpha_1 \gamma k_3 + \alpha_2 k_2 \tau) \phi_h \theta_h}{\mu_h k_2 (\mu_h k_1 k_3 - \alpha_2 \varphi \phi_h + k_1 k_3 \phi_h)} \\
 S_r^* &= \frac{\theta_r}{\mu_r + \phi_r} \\
 E_r^* &= \frac{\theta_r}{k_4 (\mu_r + \phi_r)} \\
 I_r^* &= \frac{\phi_r \alpha_3 \theta_r}{k_4 k_5 (\mu_r + \phi_r)}
 \end{aligned}
 \tag{9}$$

where $k_1 = \alpha_1 + \alpha_2 + \mu_h$, $k_2 = \mu_h + \delta_h + \gamma$, $k_3 = \varphi + \tau + \delta_h + \mu_h$, $k_4 = \mu_r + \alpha_3$, $k_5 = \mu_r + \delta_r$, $\phi_h = \frac{\beta_1 I_r^* + \beta_2 I_h^*}{N_h}$, $\phi_r = \frac{\beta_3 I_r^*}{N_r}$.

Basic reproduction number

In our proposed model 1, compartments S_h, R_h and S_r are the disease free states whereas the compartments E_h, I_h, Q_h, E_r and I_r are the infection class.

Hence the monkeypox-free equilibrium state can be given as:

$$\Phi_{MFE} = \left(\frac{\theta_h}{\mu_h}, 0, 0, 0, 0, \frac{\theta_r}{\mu_r}, 0, 0 \right) \tag{10}$$

The basic reproduction number is one of the critical parameters to examine the long-term behaviour of an epidemic. It can be defined as the number of secondary cases produced by a single infected individual in its entire life span as infectious agent. We have used next-generation matrix technique explained in Diekmann et al. (2010), Peter et al. (2020), to obtain the expression of reproduction number R_0 . It was first introduced by Driessche and Watmough van den Driessche and Watmough (2008), where this technique is discussed in detail for the estimation of R_0 . Also, there are various articles available in literature where the next-generation matrix technique has been used to estimate the expression for the basic reproduction number (Samui et al. 2020; Kumar et al. 2021).

The model system 1 can be written as:

$$\frac{dx}{dt} = \mathcal{F}(x) - \mathcal{V}(x)$$

$$\mathcal{F} = \begin{pmatrix} 0 \\ (\frac{\beta_1 I_r + \beta_2 I_h}{N_h}) S_h \\ 0 \\ 0 \\ 0 \\ 0 \\ 0 \\ 0 \end{pmatrix}$$

$$\mathcal{V} = \begin{pmatrix} -\theta_h + \frac{(\beta_1 I_r + \beta_2 I_h) S_h}{N_h} + \mu_h S_h - \varphi Q_h \\ (\alpha_1 + \alpha_2 + \mu_h) E_h \\ -\alpha_1 E_h + (\mu_h + \delta_h + \gamma) I_h \\ -\alpha_2 E_h + (\varphi + \tau + \delta_h + \mu_h) Q_h \\ -\gamma I_h - \tau Q_h + \mu_h R_h \\ -\theta_r + \frac{\beta_3 S_r I_r}{N_r} + \mu_r S_r \\ -\frac{\beta_3 S_r I_r}{N_r} + (\mu_r + \alpha_3) E_r \\ -\alpha_3 E_r + (\mu_r + \delta_r) I_r \end{pmatrix} \tag{11}$$

Progression from E_h to I_h or Q_h are not considered to be new infections, but rather the progression of infected individuals through various compartments. Hence, the transmissions matrix F and transitions matrix V can be given as :

$$F = \begin{pmatrix} 0 & \beta_2 & 0 & \beta_1 \\ 0 & 0 & 0 & 0 \\ 0 & 0 & 0 & 0 \\ 0 & 0 & 0 & 0 \end{pmatrix}$$

$$V = \begin{pmatrix} \alpha_1 + \alpha_2 + \mu_h & 0 & 0 & 0 \\ -\alpha_1 & \mu_h + \delta_h + \gamma & 0 & 0 \\ -\alpha_2 & 0 & \varphi\tau + \delta_h + \mu_h & 0 \\ 0 & 0 & 0 & \mu_r + \delta_r \end{pmatrix}$$

For simplicity, let $Y_1 = \alpha_1 + \alpha_2 + \mu_h$, $Y_2 = \mu_h + \delta_h + \gamma$, $Y_3 = \varphi\tau + \delta_h + \mu_h$ and $Y_4 = \mu_r + \delta_r$

Now:

$$V^{-1} = \frac{1}{Y_1 Y_2 Y_3 Y_4} \begin{pmatrix} Y_2 Y_3 Y_4 & 0 & 0 & 0 \\ \alpha_1 Y_3 Y_4 & Y_1 Y_3 Y_4 & 0 & 0 \\ \alpha_2 Y_2 Y_4 & 0 & Y_1 Y_2 Y_4 & 0 \\ 0 & 0 & 0 & Y_1 Y_2 Y_3 \end{pmatrix} \tag{12}$$

Now, after much simplification we obtain:

$$FV^{-1} = \frac{1}{Y_1 Y_2 Y_3 Y_4} \begin{pmatrix} \beta_2 \alpha_1 Y_3 Y_4 & 0 & 0 & \beta_1 Y_1 Y_2 Y_3 \\ 0 & 0 & 0 & 0 \\ 0 & 0 & 0 & 0 \\ 0 & 0 & 0 & 0 \end{pmatrix} \tag{13}$$

Now, the basic reproduction number is defined as the largest eigenvalue (spectral radius) of the next generation matrix FV^{-1} and can be obtained as:

$$R_0 = \rho(FV^{-1}) = \frac{\beta_2 \alpha_1 Y_3 Y_4}{Y_1 Y_2 Y_3 Y_4} = \frac{\beta_2 \alpha_1}{Y_1 Y_2} \tag{14}$$

Hence,

$$R_0 = \frac{\alpha_1 \beta_2}{(\alpha_1 + \alpha_2 + \mu_h)(\mu_h + \delta_h + \gamma)} \tag{15}$$

Stability of disease-free equilibrium

To obtain the conditions for the global stability for E_0 , we have used the approach set out in Castillo-Chavez and Song (2004), which states that if the model system can be written in the following form:

$$\frac{dX}{dt} = F(X, Z)$$

$$\frac{dZ}{dt} = G(X, Z), G(X, 0) = 0 \tag{16}$$

here $X \in R^n$ are the uninfected individuals and $Z \in R^m$ describes the infected individuals. According to this notation, the disease-free equilibrium is given by $Q_0 = (X_0, 0)$. Now, the following two conditions guarantees the global stability of the disease free equilibrium.

- K1 : For $\frac{dX}{dt} = F(X, 0)$, X_0 is globally asymptotically stable.
- K2 : $G(X, Z) = BZ - \hat{G}(X, Z)$ where $\hat{G}(X, Z) \geq 0$ for $X, Z \in \Omega$.

here $B = D_z G(X_0, 0)$ is a M -matrix and Ω is the feasible of the model. The following theorem then defines the global stability of E_0 .

Lemma 1 *The equilibrium point $Q_0 = (X_0, 0)$ is a globally asymptotically stable when $R_0 \leq 1$ and assumptions K_1 and K_2 are satisfied.*

Now, the following theorem establishes the global stability of the disease free equilibrium E_0 for our proposed model system.

Theorem 2 *The DFE point E_0 is globally asymptotically stable provided $R_0 \leq 1$.*

Proof First, we will prove K_1 as:

$$F(X, 0) = \begin{bmatrix} \theta_h - \mu_h S_h \\ -\mu_h R_h \\ \theta_r - \mu_r S_r \\ -(\mu_r + \alpha_3)E_r \end{bmatrix}$$

The characteristic polynomial of $F(X, 0)$ is:

$$(\lambda + \mu_h)^2(\lambda + \mu_r)(\lambda + \mu_r + \alpha_3) \tag{17}$$

$\Rightarrow \lambda_1 = \lambda_2 = -\mu_h, \lambda_3 = -\mu_r$ and $\lambda_4 = -\mu_r - \alpha_3$.
Hence, $X = X_0$ is globally asymptotically stable.
Now, we have:

$$G(X, Z) = BZ - \hat{G}(X, Z) \tag{18}$$

$$= \begin{bmatrix} -(\alpha_1 + \alpha_2 + \mu_h) & \frac{\beta_2 S_h^0}{N_h} & 0 & \frac{\beta_1 S_h^0}{N_h} \\ \alpha_1 & -(\mu_h + \delta_h + \gamma) & 0 & 0 \\ \alpha_2 & 0 & -(\varphi + \tau + \delta_h + \mu_h) & 0 \\ 0 & 0 & 0 & \mu_r + \delta_r \end{bmatrix} \times \begin{bmatrix} E_h \\ I_h \\ Q_h \\ I_r \end{bmatrix} - \begin{bmatrix} (\frac{\beta_2(S_h^0 - S_h) + \beta_1(S_h^0 - S_h)}{N_h})E_h \\ 0 \\ 0 \\ \alpha_3 E_r \end{bmatrix} \tag{19}$$

Here, one can easily observe that B satisfies all conditions explained in K2. \square

Stability of endemic equilibrium

We will use the Routh–Hurwitz criterion to prove the local stability of the endemic equilibria. Here, we will derive the conditions under which the endemic equilibria is locally asymptotically stable.

The Jacobian matrix about the endemic equilibria ϕ_{MEE} is given as :

$$J = \begin{bmatrix} a_{11} & 0 & a_{13} & a_{14} & 0 & 0 & 0 & a_{18} \\ a_{21} & a_{22} & a_{23} & 0 & 0 & 0 & 0 & a_{28} \\ 0 & a_{32} & a_{33} & 0 & 0 & 0 & 0 & 0 \\ 0 & a_{42} & 0 & a_{44} & 0 & 0 & 0 & 0 \\ 0 & 0 & a_{53} & a_{54} & a_{55} & 0 & 0 & 0 \\ 0 & 0 & 0 & 0 & 0 & a_{66} & 0 & a_{68} \\ 0 & 0 & 0 & 0 & 0 & a_{76} & a_{77} & a_{78} \\ 0 & 0 & 0 & 0 & 0 & 0 & a_{87} & a_{88} \end{bmatrix}$$

Here,

$$\begin{aligned} a_{11} &= -\left(\frac{\beta_1 I_r + \beta_2 I_h}{N_h}\right) - \mu_h & a_{13} &= -\frac{\beta_2 S_h}{N_h} \\ a_{14} &= \phi & a_{18} &= -\frac{\beta_1 S_h}{N_h} \\ a_{21} &= \frac{\beta_1 I_r + \beta_2 I_h}{N_h} & a_{22} &= -(\alpha_1 + \alpha_2 + \mu_h) \\ a_{23} &= \frac{\beta_2 S_h}{N_h} & a_{28} &= \frac{\beta_1 S_h}{N_h} \\ a_{32} &= \alpha_1 & a_{33} &= -(\mu_h + \delta_h + \gamma) \\ a_{42} &= \alpha_2 & a_{44} &= -(\varphi + \tau + \delta_h + \mu_h) \\ a_{53} &= \gamma & a_{54} &= \tau & a_{55} &= -\mu_h \\ a_{66} &= -(\mu_r + \frac{\beta_3 I_r}{N_r}) & a_{68} &= -\frac{\beta_3 S_r}{N_r} \\ a_{76} &= \frac{\beta_3 I_r}{N_r} & a_{77} &= -(\mu_r + \alpha_3) \\ a_{78} &= \frac{\beta_3 S_r}{N_r} & a_{87} &= \alpha_3 & a_{88} &= -(\mu_r + \delta_r) \end{aligned}$$

The characteristic equation of J is given as:

$$\frac{1}{N_h N_r} \left[(-x - \mu_h)(-\phi\alpha_2(I_r\beta_1 + I_h\beta_2)(x + \gamma + \delta_h + \mu_h) + (-x - \tau - \varphi - \delta_h - \mu_h)(S_h\alpha_1\beta_2(x + \mu_h) - (x + \alpha_1 + \alpha_2 + \mu_h)(x + \gamma + \delta_h + \mu_h)(I_r\beta_1 + I_h\beta_2 + N_h(x + \mu_h)))) \right. \\ \left. (S_r\alpha_3\beta_3(x + \mu_r) - (x + \alpha_3 + \mu_r)(I_r\beta_3 + N_r(x + \mu_r)))(x + (\mu_r + \delta_r)) \right] = 0 \tag{20}$$

which can be further written as:

$$x^8 + A_1x^7 + A_2x^6 + A_3x^5 + A_4x^4 + A_5x^3 + A_6x^2 + A_7x + A_8 = 0 \tag{21}$$

where A_i 's are the coefficients of $x^{8-i}; i = 1, 2, \dots, 8$ after converting the polynomial in standard form.

Note: To obtain the condition for the stability of ϕ_{MEE} we will made the following substitution:

$$\begin{aligned}
 P &= \frac{A_1A_2 - A_0A_3}{A_1}, & Q &= \frac{A_1A_4 - A_0A_5}{A_1}, \\
 R &= \frac{A_1A_6 - A_0A_7}{A_1}, & S &= A_8, \\
 P^* &= \frac{pA_3 - A_1Q}{P}, & Q^* &= \frac{PA_5 - A_1R}{P}, \\
 R^* &= \frac{PA_7 - A_1S}{P}, & M &= \frac{P^*Q - PQ^*}{P^*}, \\
 N &= \frac{P^*R - PR^*}{P^*}, & T &= \frac{P^*S}{P^*}, \\
 M^* &= \frac{MQ^* - P^*N}{M}, & N^* &= \frac{MR^* - P^*T}{M}, \\
 X &= \frac{M^*N - MN^*}{M^*}.
 \end{aligned}$$

Hence, we can conclude this section by the following theorem:

Theorem 3 *The endemic equilibrium point ϕ_{MEE} is locally asymptotically stable provided $R_0 > 1$ and following conditions are satisfied:*

$$\begin{aligned}
 A_1 &> 0, \\
 A_1A_2 &> A_3, \\
 A_1A_2A_3 + A_0A_1A_5 &> A_0A_3^2 + A_1^2A_4 \\
 P^*Q &> PQ^* \quad MQ^* > P^*N \quad M^*N > MN^* \quad XN^* > TM^*
 \end{aligned} \tag{22}$$

Backward bifurcation

The analysis conducted in the previous section on the occurrence of endemic equilibrium E^* suggests the probability of backward bifurcation. It can be defined as the state when a stable endemic equilibrium coexist with with a stable disease-free equilibrium when the associated reproduction number is less than unity. We use the center manifold based result (theorem 4.1) given in Castillo-Chavez and Song (2004), to check the occurrence of backward bifurcation.

Let:

$$\begin{aligned}
 S_h &= y_1, & E_h &= y_2, & I_h &= y_3, & Q_h &= y_4, \\
 R_h &= y_5, & S_r &= y_6, & E_r &= y_7, & I_r &= y_8.
 \end{aligned}$$

Consider, $U = (y_1, y_2, y_3, y_4, y_5, y_6, y_7, y_8)^T$, then the given system (1) can be written as:

$$\frac{dU}{dt} = (f_1, f_2, f_3, f_4, f_5, f_6, f_7, f_8)^T \tag{23}$$

where,

$$\begin{aligned}
 f_1 &= \theta_h - \frac{(\beta_1y_8 + \beta_2y_3)S_h}{N_h} - \mu_hy_1 + \phi y_4 \\
 f_2 &= \frac{(\beta_1y_8 + \beta_2y_3)S_h}{N_h} - (\alpha_1 + \alpha_2 + \mu_h)y_2 \\
 f_3 &= \alpha_1y_2 - (\mu_h + \delta_h + \gamma)y_3 \\
 f_4 &= \alpha_2y_2 - (\varphi + \tau + \delta_h + \mu_h)y_4 \\
 f_5 &= \gamma y_3 + \tau y_4 - \mu_hy_5 \\
 f_6 &= \theta_r - \frac{\beta_3y_6y_8}{N_r} - \mu_r y_6 \\
 f_7 &= \frac{\beta_3y_6y_8}{N_r} - (\mu_r + \alpha_3)y_7 \\
 f_8 &= \alpha_3y_7 - (\mu_r + \delta_r)y_8
 \end{aligned} \tag{24}$$

From the expression of R_0 , we can observe that R_0 is highly influenced by β_2 , the product of effective contact rate and the probability of human been infected with monkey pox virus after getting in contact with infectious human. Therefore, we will consider β_2 as our bifurcation parameter.

Hence , when $R_0 = 1$, we have:

$$\beta_2^* = \frac{(\alpha_1 + \alpha_2 + \mu_h)(\mu_h + \delta_h + \gamma)}{\alpha_1} \tag{25}$$

Now, the above system at monkeypox-free equilibrium state ϕ_{MFE} is given by:

$$J_0(\phi_{MFE}, \beta_2^*) = \begin{bmatrix} -\mu_h & 0 & -\beta_2 & 0 & 0 & 0 & 0 & -\beta_1 \\ 0 & -A_1 & \beta_2 & 0 & 0 & 0 & 0 & \beta_1 \\ 0 & \alpha_1 & -A_2 & 0 & 0 & 0 & 0 & 0 \\ 0 & \alpha_2 & 0 & -A_3 & 0 & 0 & 0 & 0 \\ 0 & 0 & \gamma & \tau & -\mu_h & 0 & 0 & 0 \\ 0 & 0 & 0 & 0 & 0 & -\mu_r & 0 & 0 \\ 0 & 0 & 0 & 0 & 0 & 0 & -A_4 & \beta_3 \\ 0 & 0 & 0 & 0 & 0 & 0 & \alpha_3 & -A_5 \end{bmatrix}$$

Clearly, ‘0’ is an eigenvalue of $J_0(\phi_{MFE}, \beta_2^*)$. Let $W = (w_1, w_2, w_3, w_4, w_5, w_6, w_7, w_8)$ be the associated right eigenvector corresponding to zero eigenvalue, and can be attained by simplifying:

$$\begin{aligned}
 -\mu_hw_1 - \beta_2w_3 - \beta_1w_8 &= 0 \\
 -A_1w_2 + \beta_2w_3 + \beta_1w_8 &= 0 \\
 \alpha_1w_2 - A_2w_3 &= 0 \\
 \alpha_2w_2 - A_3w_4 &= 0 \\
 \gamma w_3 + \tau w_4 - \mu_hw_5 &= 0 \\
 -\mu_rw_6 - \beta_3w_8 &= 0 \\
 -A_4w_7 + \beta_3w_8 &= 0 \\
 \alpha_3w_7 - A_5w_8 &= 0
 \end{aligned} \tag{26}$$

On evaluation, W can be given as:

$$\begin{aligned}
 w_1 &= -\frac{A_1 A_2}{\alpha_1 \mu_h} & w_2 &= \frac{A_2}{\alpha_1} & w_3 &= 1 \\
 w_4 &= \frac{\alpha_2 A_2}{\alpha_1 A_3} & w_5 &= \frac{1}{\mu_h} \left(\gamma + \frac{\tau \alpha_2 A_2}{\alpha_1 A_3} \right) \\
 w_6 &= \frac{\beta_3}{\beta_1 \mu_r} \left(\frac{A_1 A_2}{\alpha_1} + \beta_2 \right) \\
 w_7 &= -\frac{A_5}{\alpha_3 \beta_1} \left(\frac{A_1 A_2}{\alpha_1} + \beta_2 \right) & w_8 &= -\frac{1}{\beta_1} \left(\frac{A_1 A_2}{\alpha_1} + \beta_2 \right)
 \end{aligned}$$

Now, let $V = (v_1, v_2, v_3, v_4, v_5, v_6, v_7, v_8)$ be the associated left eigenvector of J_0 corresponding to zero eigenvalue and satisfying $V \cdot W = 0$. Then V can be given as :

$$\begin{aligned}
 v_1 &= 0, \\
 v_2 &= \left(\frac{A_2}{\alpha_1} + \frac{\beta_2}{A_2} - \left(\frac{A_1 A_3}{\alpha_1} + \beta_2 \right) \cdot \frac{1}{\left(\frac{A_4 A_5}{\alpha_3} - \beta_3 \right)} \times \left(\frac{A_5}{\alpha_3} + \frac{\beta_2}{A_2} \right) \right)^{-1}, \\
 v_3 &= \frac{\beta_2}{A_2} \cdot v_2, & v_4 &= v_5 = v_6 = 0, \\
 v_7 &= \frac{\beta_1}{\left(\frac{A_4 A_5}{\alpha_3} - \beta_3 \right)} \cdot v_2, & v_8 &= \frac{\beta_2}{A_2} \cdot v_7
 \end{aligned}$$

As discussed in theorem 4.1 (Castillo-Chavez and Song 2004), we have:

$$a = \sum_{k,i,j=1}^8 v_k w_i w_j \frac{\partial^2 f_k}{\partial y_i \partial y_j} (\phi_{MFE}, \beta_2^*) \tag{27}$$

$$b = \sum_{k,i=1}^8 v_k w_i \frac{\partial^2 f_k}{\partial y_i \partial \beta_2} (\phi_{MFE}, \beta_2^*) \tag{28}$$

Algebraic calculations shows that:

$$\begin{aligned}
 \frac{\partial^2 f_2}{\partial x_1 \partial x_3} &= \frac{\beta_2}{N_h} = \frac{\partial^2 f_2}{\partial x_3 \partial x_1} & \frac{\partial^2 f_2}{\partial x_1 \partial x_8} &= \frac{\beta_1}{N_h} = \frac{\partial^2 f_2}{\partial x_8 \partial x_1} \\
 \frac{\partial^2 f_7}{\partial x_8 \partial x_6} &= \frac{1}{N_r} = \frac{\partial^2 f_7}{\partial x_6 \partial x_8}
 \end{aligned}$$

Now, substituting all the above values in the expressions for ‘a’ and ‘b’, we obtain:

$$a = \frac{2v_2 w_1}{N_h} (w_3 \beta_2 + w_8 \beta_1) + 2v_7 \frac{w_6 w_8}{N_r} \tag{29}$$

$$b = v_2 \cdot w_2 \cdot \frac{\theta}{\mu_h N_h} \tag{30}$$

Now, to persist backward bifurcation in the proposed model, both the values of ‘a’ and ‘b’ has to be simultaneously positive.

Results

A sensitivity analysis determines how different values of an independent variable affect a particular dependent variable under a given set of assumptions (Kalyan et al. 2021; Victorr et al. 2020). The normalized forward sensitivity index of a variable to a parameter is the ratio of the relative change in the variable to the relative change in the parameter. When variable is a differentiable function of the parameter, the sensitivity index may be alternatively defined using partial derivatives. The parameter values have been taken from literature as given in Table 1.

Since the basic reproduction number R_0 helps us to predict the future course of the disease, the sensitivity analysis is performed to understand which parameters involved in the model effect the value of R_0 relatively more. We have used the following expression of the sensitivity for R_0 which depends upon parameter v .

$$\psi_v^{R_0} = \frac{v}{R_0} \times \frac{\partial R_0}{\partial v} \tag{31}$$

A negative index of sensitivity shows that the parameter and R_0 are inversely proportional. A positive sensitivity index, however, denotes that the value of R_0 increases with an increase in the value of the parameter concerned.

The estimated sensitivity indices for R_0 are presented in Table 2. From Table 2, we can see that an increase in the values of α_2 , μ_h , δ_h and γ will results in a decrease in the value of R_0 . On the another hand, an increase in the value of α_1 and β_2 will increase the monkey-pox cases.

Table 2 Sensitivity index of parameters

Parameter	Expression of the sensitivity index	Value
α_1	$\frac{\alpha_2 + \mu_h}{\alpha_1 + \alpha_2 + \mu_h}$	0.945946
α_2	$-\frac{\alpha_2}{\alpha_1 + \alpha_2 + \mu_h}$	- 0.540541
β_2	1	1
μ_h	$-\frac{\mu_h (\gamma + \alpha_1 + \alpha_2 + \delta_h + 2\mu_h)}{(\alpha_1 + \alpha_2 + \mu_h)(\gamma + \delta_h + \mu_h)}$	- 0.998291
δ_h	$-\frac{\delta_h}{\gamma + \delta_h + \mu_h}$	- 0.0790514
γ	$-\frac{\gamma}{\gamma + \delta_h + \mu_h}$	- 0.328063

Discussion

The basic reproduction number is a crucial parameter in disease dynamics which gives us major information about the disease. To understand the effect of various disease transmission parameters on the basic reproduction number, we have obtained the surface plots showing variation of R_0 with sensitive parameters. From Fig. 2, it can be observed that as the value of α_2 increases, it leads to reduced disease transmission. Similarly, it can be easily seen from Fig. 3 that contact rate with rodent population directly affects the transmission of monkey-pox. Similarly, the simultaneous effect of β_2 , α_2 , μ_h and γ on the basic reproduction number has been shown in Figs. 4 and 5.

Further, we have performed numerical experiments to detect effect of change in sensitive parameters on the number of infected individuals. This has been investigated in Figs. 6, 7 and 8. Now we have incorporated a compartment

Q_h in the model, which consists of the isolated proportion of the infected humans. Through numerical simulations, we have shown how the infected population would behave in the absence of isolated interventions. In Fig. 9, we show that the isolation of infected individuals helps to reduce disease transmission.

Conclusion

A non-linear compartmental model has been proposed to understand the transmission of Monkey pox disease. The proposed model consist of eight mutually exclusive compartments. The human population has been divided into five compartments, where we has introduced the exposed (E_h) and isolated human (Q_h) compartments along with standard compartments of exposed population (E_h), infected humans (I_h) and recovered humans (R_h). Similarly, the rodent population is also divided into three compartments; exposed

Fig. 2 Surface plot showing simultaneous impact of α_1 and α_2 on R_0

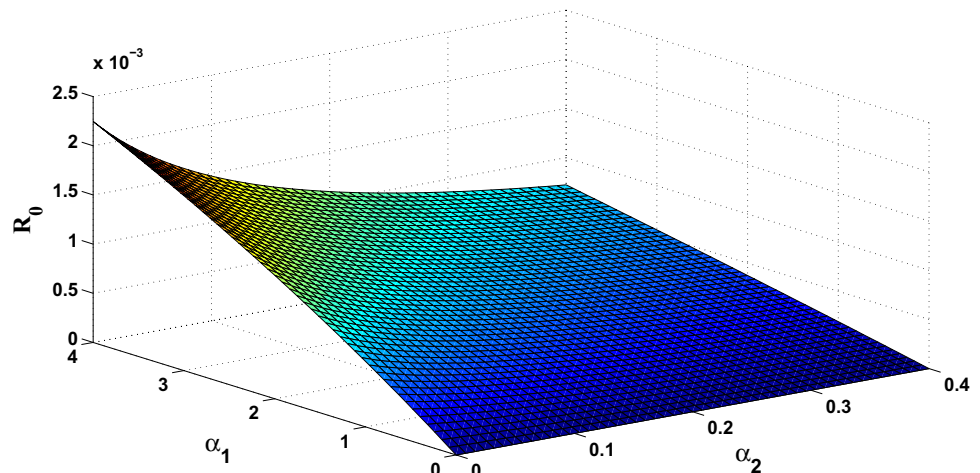


Fig. 3 Surface plot showing simultaneous impact of α_1 and β_2 on R_0

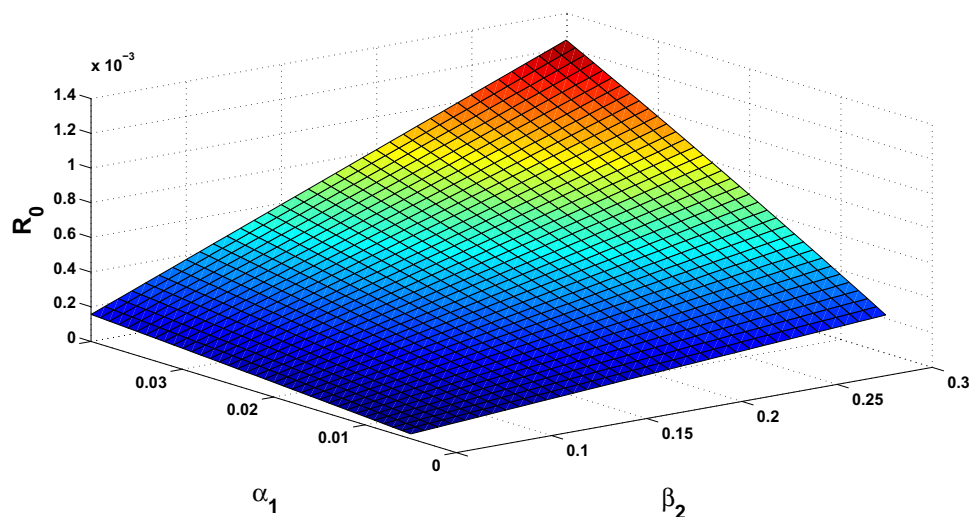


Fig. 4 Surface plot showing simultaneous impact of β_2 and α_2 on R_0

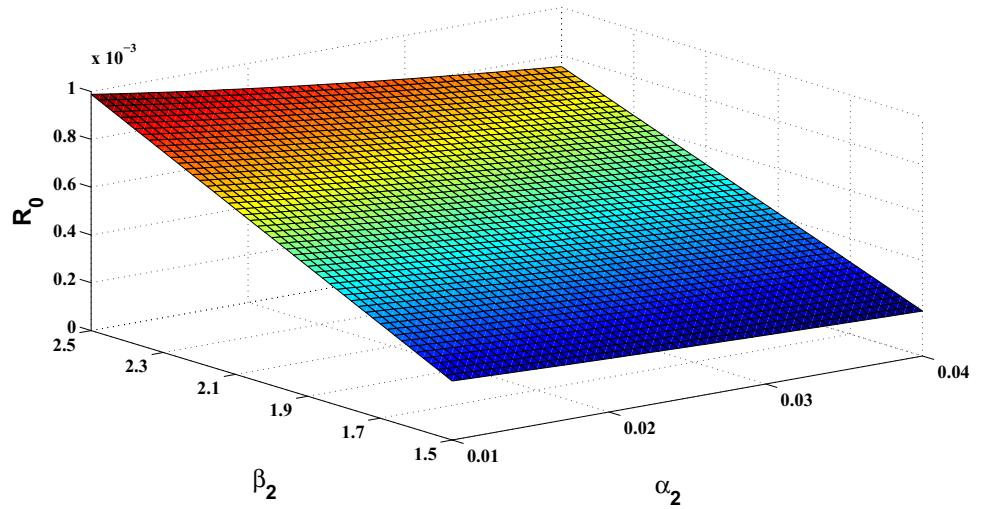


Fig. 5 Surface plot showing simultaneous impact of μ_h and γ on R_0

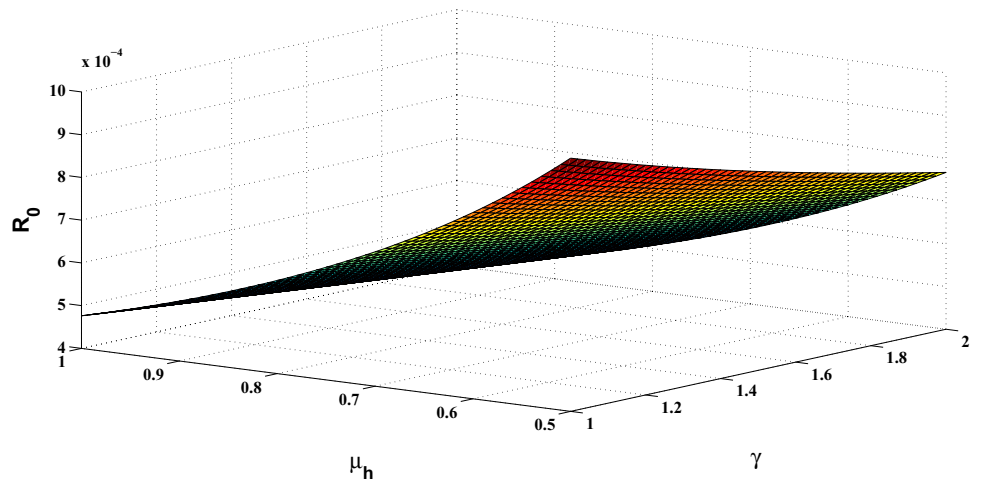
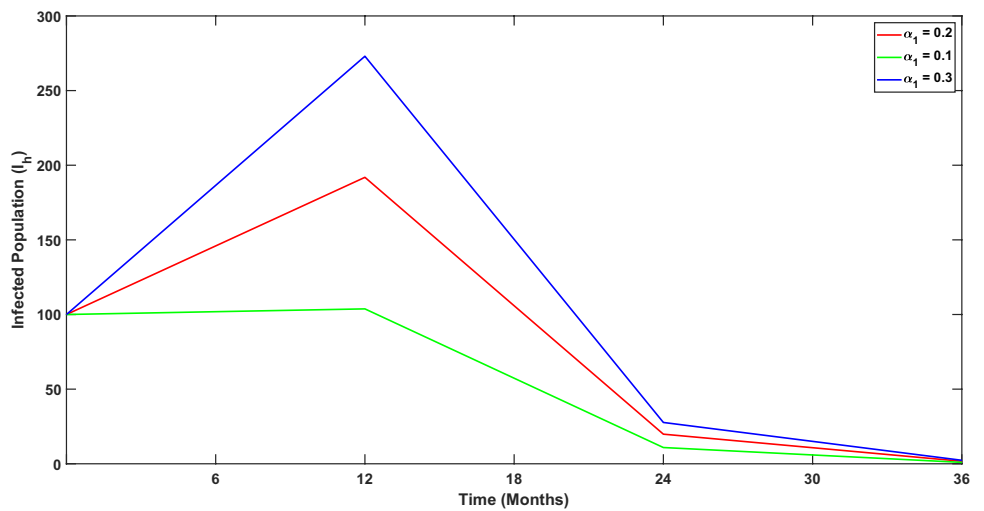


Fig. 6 Variation in infected population over time for different values of α_1 ; proportion of humans exposed to infection



(E_r), susceptible (S_r) and infected rodents (I_r). Further, we have established the fundamental properties of the proposed model.

Basic reproduction number has been estimated using next-generation matrix technique. The proposed model exhibit two equilibrium points; disease free equilibrium

Fig. 7 Variation in infected population over time for different values of δ_h ; disease induced death rate of humans

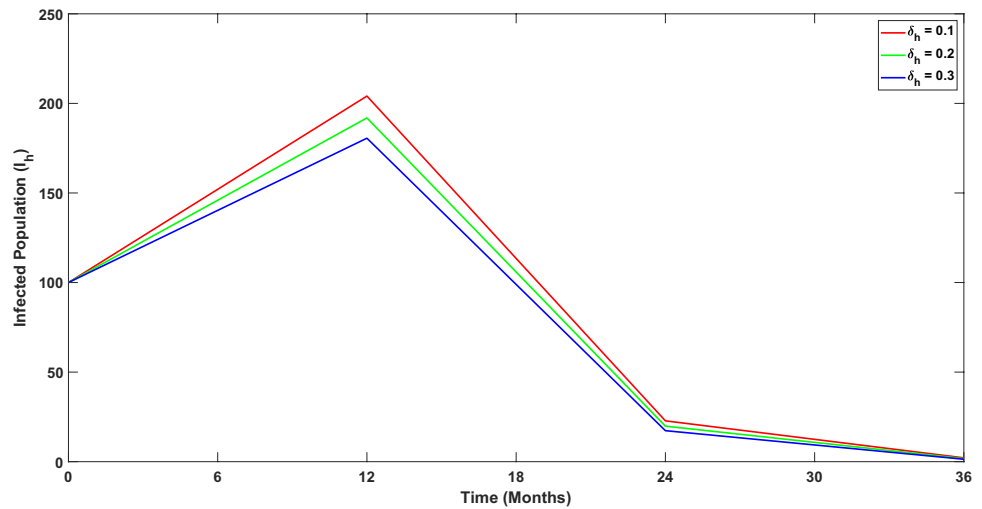


Fig. 8 Variation in infected population over time for different values of γ ; recovery rate of humans

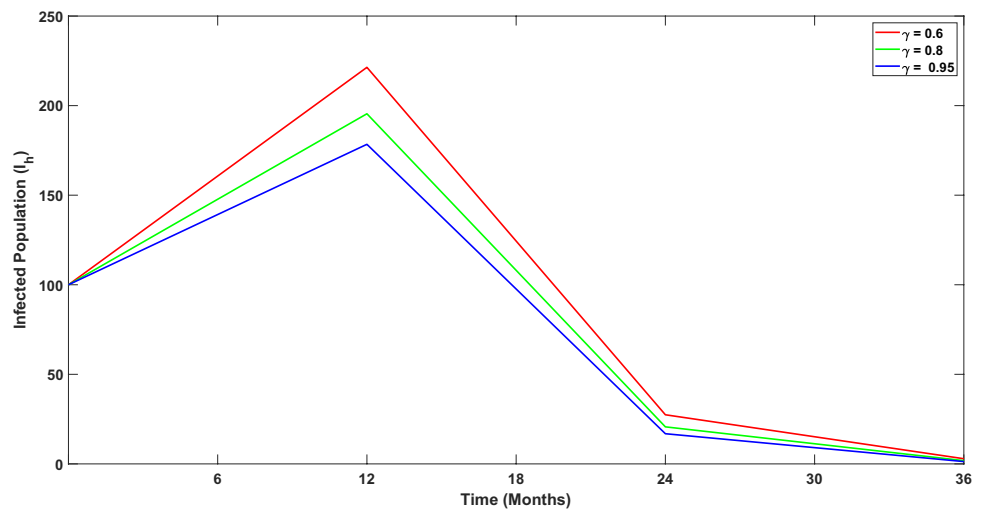
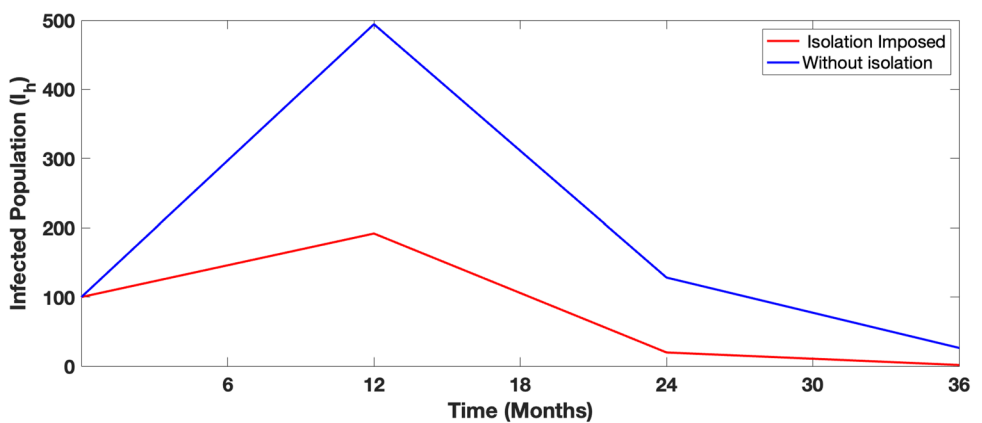


Fig. 9 Variation in infected population without any isolated interventions



point and endemic equilibrium point. We have obtained the stability conditions for both of the equilibrium points. Further, the existence of the endemic equilibrium implies the possibility of the backward bifurcation. We have also derived the condition for the existence of the backward

bifurcation. Further we have shown the sensitivity of various parameters involved in the model. The sensitivity index has been provided in Table 2. We found that α_2 , which is human to human contact rate is the most sensitive parameter in the transmission of the disease. Also, with the help of numerical

simulations, we have shown the simultaneous effect of various parameters on the basic reproduction number R_0 . Our analysis suggests that isolation of infected humans helps to reduce disease transmission. It is, therefore, realised from the simulation that isolation of the infected humans, is playing significant roles in the management and control of monkeypox virus.

References

- Alakunle E, Moens U, Nchinda G, Okeke M (2020) Monkeypox virus in Nigeria: infection biology, epidemiology, and evolution. *Viruses* 12(11):1257
- Bankuru SV, Kossol S, Hou W, Mahmoudi P, Rychtář J, Taylor D (2020) A game-theoretic model of monkeypox to assess vaccination strategies. *PeerJ* 8:e9272
- Bhunu C, Garira W, Magombedze G (2009) Mathematical analysis of a two strain hiv/aids model with antiretroviral treatment. *Acta Biotheor* 57(3):361–381
- Bhunu C, Mushayabasa S (2011) Modelling the transmission dynamics of pox-like infections. *IAENG Int J* 41(2):1–9
- Castillo-Chavez C, Song B (2004) Dynamical models of tuberculosis and their applications. *Math Biosci Eng* 1(2):361
- CDC (2003) What you should know about monkeypox. <https://www.cdc.gov/poxvirus/monkeypox/>
- Diekmann O, Heesterbeek J, Roberts MG (2010) The construction of next-generation matrices for compartmental epidemic models. *J R Soc Interface* 7(47):873–885
- Durski KN, McCollum AM, Nakazawa Y, Petersen BW, Reynolds MG, Briand S, Djingarey MH, Olson V, Damon IK, Khalakdina A (2018) Emergence of monkeypox-west and central africa, 1970–2017. *Morb Mortal Wkly Rep* 67(10):306
- Emeka P, Ounorah M, Eguda F, Babangida B (2020) Mathematical model for monkeypox virus transmission dynamics. *Epidemiol Open Access* 8(3):1000348
- Grant R, Nguyen L-BL, Breban R (2020) Modelling human-to-human transmission of monkeypox. *Bull World Health Organ* 98(9):638
- Hutson CL, Gallardo-Romero N, Carroll DS, Clemmons C, Salzer JS, Nagy T, Hughes CM, Olson VA, Karem KL, Damon IK (2013) Transmissibility of the monkeypox virus clades via respiratory transmission: investigation using the prairie dog-monkeypox virus challenge system. *PLoS ONE* 8(2):e55488
- Jezeq Z, Szczeniowski M, Paluku K, Mutombo M, Grab B (1988) Human monkeypox: confusion with chickenpox. *Acta Trop* 45(4):297–307
- Kalyan D, Reddy KG, Lakshminarayan K (2021) Sensitivity and elasticity analysis of novel corona virus transmission model: a mathematical approach. *Sensors Int* 2(1):100088
- Kantele A, Chickering K, Vapalahti O, Rimoin A (2016) Emerging diseases-the monkeypox epidemic in the democratic republic of the congo. *Clin Microbiol Infect* 22(8):658–659
- Kumar S, Sharma S, Singh F, Bhatnagar P, Kumari N (2021) A mathematical model for COVID-19 in Italy with possible control strategies. *Mathematical analysis for transmission of COVID-19*, p 101
- Ladnyj I, Ziegler P, Kima E (1972) A human infection caused by monkeypox virus in basankusu territory, democratic Republic of the Congo. *Bull World Health Organ* 46(5):593
- Meyer H, Ehmann R, Smith GL (2020) Smallpox in the post-eradication era. *Viruses* 12(2):138
- Nguyen P, Ajisegiri W, Costantino V, Chughtai A, MacIntyre C (2021) Reemergence of human monkeypox and declining population immunity in the context of urbanization, Nigeria, 2017–2020. *Emerg Infect Dis* 27(4):1007–1014
- Odom MR, Curtis Hendrickson R, Lefkowitz EJ (2009) Poxvirus protein evolution: family wide assessment of possible horizontal gene transfer events. *Virus Res* 144:233–249
- Peter O, Viriyapong R, Oguntolu F, Yosyingyong P, Edogbanya H, MO A (2020) Stability and optimal control analysis of an scir epidemic model. *J Math Comput Sci* 2020(1):2722–2753
- Rimoin AW, Mulembakani PM, Johnston SC, Smith JOL, Kivalu NK, Kinkela TL, Blumberg S, Thomassen HA, Pike BL, Fair JN et al (2010) Major increase in human monkeypox incidence 30 years after smallpox vaccination campaigns cease in the democratic republic of congo. *Proc Natl Acad Sci* 107(37):16262–16267
- Samui P, Mondal J, Khajanchi S (2020) A mathematical model for COVID-19 transmission dynamics with a case study of India. *Chaos Solit Fract* 140:110173
- Somma S, Akinwande N, Chado U (2019) A mathematical model of monkey pox virus transmission dynamics. *IFE J Sci* 21(1):195–204
- TeWinkel RE (2019) Stability analysis for the equilibria of a monkeypox model. Thesis and Dissertations: University of Wisconsin. <https://dc.uwm.edu/etd/2132>
- Usman S, Adamu II et al (2017) Modeling the transmission dynamics of the monkeypox virus infection with treatment and vaccination interventions. *J Appl Math Phys* 5(12):2335
- van den Driessche P, Watmough J (2008) Further notes on the basic reproduction number. Springer, Berlin, Heidelberg, pp 159–178
- Victorr Y, Hasifa N, Julius T (2020) Analysis of the model on the effect of seasonal factors on malaria transmission dynamics. *J Appl Math* 2020(4):19

Publisher's Note Springer Nature remains neutral with regard to jurisdictional claims in published maps and institutional affiliations.